ChemComm

COMMUNICATION

View Article Online
View Journal | View Issue

Cite this: *Chem. Commun.*, 2026, **62**, 6577

Received 6th December 2025,
Accepted 3rd March 2026

DOI: 10.1039/d5cc06960b

rsc.li/chemcomm

Unveiling a host–guest assembly composed of an emissive Ir(III) complex salt and a concave aromatic host at a local minimum state

Shota Ogura,[a] Kanami Sugiyama,[b] Masahiro Higashi [c] and Shinnosuke Horiuchi *[a]

A host–guest complex formed at a local minimum state was isolated and characterized. Owing to solubility modulation induced by the formation of a supramolecular assembly, the host–guest complex at a local minimum state selectively precipitated. The photophysical properties of the guest gave structural information about local environments around the guest in the solid state.

The self-assembly process is governed by thermodynamics, and thus the thermodynamically favored structure located at the global minimum on the energy landscape is obtained as the predominant product through self-assembly. This process provides a rational synthetic methodology for constructing three-dimensional giant structures with unique functionalities, contributing to the development of supramolecular chemistry.[1,2] In contrast, some biological systems consume energy and chemical fuels through irreversible processes to move from the global minimum state to a local minimum state, exhibiting important biological functions such as cell division, motility, and signal transduction.[3] To construct such dissipative molecular systems, recent studies in supramolecular chemistry have focused on developing unique supramolecular systems that exhibit drastic changes in the chemical and/or physical properties of assemblies *via* reversible transitions between global and local minimum states on the energy landscape.[4] From this viewpoint, understanding the structures and properties of supramolecular assemblies at local minimum states is of great importance.

The self-assembly of calixresorcin[4]arene **1** has attracted much attention owing to its unique dynamic behaviors, such as capsule formation,[5] guest recognition,[6] and catalytic activity.[7] These characteristics originate from the concerted effects of weak noncovalent interactions, including hydrogen bonds, cation–π, CH–π, and Coulombic interactions between the components, which are reminiscent of natural enzymatic systems. During the encapsulation process, the hexameric structure of $\mathbf{1}_6$ is kinetically stabilized by multiple hydrogen bonds involving additional water molecules. Consequently, guest encapsulation within $\mathbf{1}_6$ is accelerated under heating conditions, as the dissociation of a monomer unit **1** from $\mathbf{1}_6$ is promoted to create a transient portal in the capsule framework.[6b] When sterically hindered guests are used, the encapsulation proceeds more slowly, allowing the observation of a metastable (local minimum) state. Under these conditions, the encapsulation process of large guests into the internal cavity of $\mathbf{1}_6$ can be discussed (Fig. 1).[8] Our group found that the thermodynamic stability of host–guest complexes composed of the hydrogen-bonded capsule $\mathbf{1}_6$ and cationic Iridium(III) complex with an octahedral-shaped coordination geometry, $[Ir(ppy)_2(bpy)]^+$ ($[\mathbf{2}]^+$, ppy = 2-phenyl pyridinato, bpy = 2,2′-bipyridine), depends on the counter anion of $[\mathbf{2}]^+$, as revealed by monitoring the modulation of the photophysical properties of $[\mathbf{2}]^+$ upon encapsulation.[9] This result indicates that the anion participates in the assembly process.[8,10] The delicate balance of multiple noncovalent interactions perturbed by the steric effect of guests promotes the formation of a unique symmetry-breaking host–guest assembly that exhibits enhanced chiroptical properties in solution.[11]

In this study, we further investigated the self-assembly and encapsulation processes by monitoring a metastable host–guest complex composed of **1** and $[\mathbf{2}]^+$, which is formed at a local minimum state (Fig. 2). We previously found that a mixture of free $\mathbf{1}_6$ and free $[\mathbf{2}]^+$ temporarily provided a metastable state upon mixing their solutions at room temperature (Fig. 2b). Host–guest complexes of **1** and $[\mathbf{2}]^+$ formed in the metastable state are expected to exhibit different solubility characteristics, enabling the isolation of a metastable assembly by precipitation from solution. Because precipitation is a common isolation and purification technique in materials

[a] *Department of Basic Science, Graduate School of Arts and Sciences, The University of Tokyo, 3-8-1 Komaba, Meguro-ku, Tokyo 153-8902, Japan. E-mail: shoriuchi@g.ecc.u-tokyo.ac.jp*
[b] *Department of Molecular Engineering, Graduate School of Engineering, Kyoto University, Kyoto Daigaku-Katsura, Nishikyo-ku, Kyoto 615–8510, Japan*
[c] *Department of Complex Systems Science, Graduate School of Informatics, Nagoya University, Furo-sho, Chikusa-ku, Nagoya 464–8601, Japan*

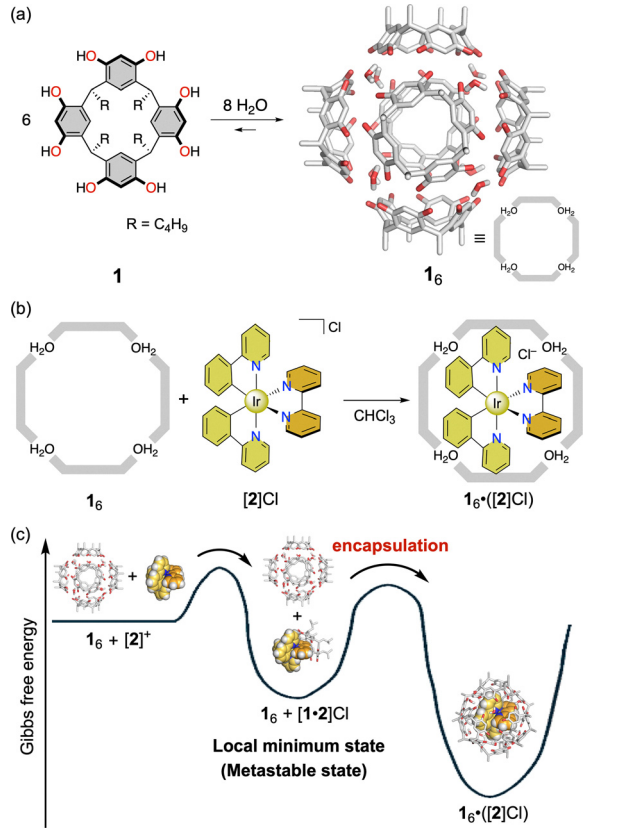

Fig. 1 Schematic representation of (a) self-assembly of **1**, and (b) encapsulation of [**2**]Cl within $\mathbf{1}_6$. (c) Energy landscape of the encapsulation process. In the equilibrium system, the mixture of **1** and $[\mathbf{2}]^+$ affords local minimum states owing to the dynamic characteristics of $\mathbf{1}_6$.

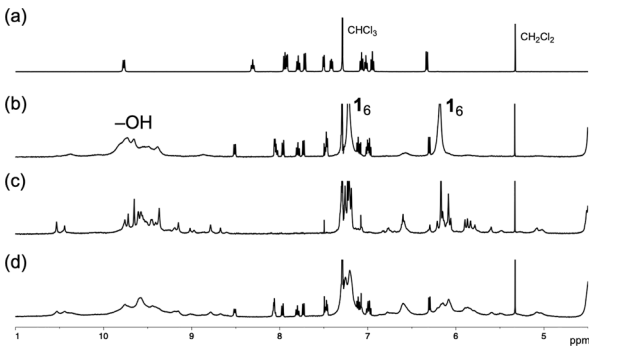

Fig. 2 ^{1}H NMR spectra (500 MHz, $CDCl_3$, r.t.) of (a) [**2**]Cl, (b) and (c) a mixture of **1** and [**2**]Cl in a 6 : 1 ratio (b) before heating (metastable state) and (c) after heating at 50 °C for 1 h (global minimum state), and (d) a mixture of **1** and [**2**]Cl in a 6 : 2 ratio after heating.

science, the least soluble species in a mixture can be obtained selectively through this process. This simple method offers a significant advantage for isolating unique assemblies, as precipitation can completely shift the equilibrium state, even when such assemblies are formed in solution as minor products. Moreover, the photophysical properties of $[\mathbf{2}]^+$ in the isolated assembly as a precipitate can give structural information about the local environment surrounding $[\mathbf{2}]^+$. This finding offers a simple approach to isolating metastable species from mixtures and provides insight into the unique structures formed at local minima on the energy landscape, governed by the characteristics of the guest.

First, we tried to obtain a host–guest assembly composed of **1** and $[\mathbf{2}]^+$ formed at a global minimum state *via* precipitation. To increase the crystallinity of the assembly, the resorcin[4]arene unit **1** bearing short alkyl rims (R = C_4H_9) was used in this study instead of the longer-rimmed analogue (R = $C_{11}H_{23}$) used in our previous studies.[9,11] As the Ir(III) complex salt is poorly soluble in *n*-hexane, precipitation of an assembly at a global minimum state was expected upon addition of *n*-hexane to a $CHCl_3$ solution of $\mathbf{1}_6$·([**2**]Cl) (Fig. 2c). However, no precipitation occurred even after several days, indicating that the Ir(III) complex cation $[\mathbf{2}]^+$ acquired solubility in *n*-hexane through encapsulation within the hydrogen-bonded hexameric capsule $\mathbf{1}_6$. Judging from the structure of host–guest complex $\mathbf{1}_6$·([**2**]Cl) formed at the global minimum state, this enhanced solubility of $[\mathbf{2}]^+$ can be attributed to the isolation of the cationic species from the solvent sphere by the resorcin[4]arene units with the alkyl chains located on the outer surface of the capsule, resulting in a micelle-like supramolecular structure.

Next, to reproduce a local minimum state, precipitation experiments were conducted using a 6 : 2 mixture of **1** and [**2**]Cl, in which approximately half of the Ir(III) complex salt is located outside the hexameric capsule in solution, resembling the metastable state (Fig. 2b and d). Upon addition of *n*-hexane to the solution, a yellow precipitate was obtained. As the host–guest complex $\mathbf{1}_6$·([**2**]Cl) does not precipitate by the addition of *n*-hexane as shown above, the isolated solid can be attributed to the metastable species. Interestingly, the ^{1}H NMR spectrum of the yellow solid revealed a 1 : 1 stoichiometric ratio of **1** and [**2**]Cl, rather than pure [**2**]Cl (Fig. S1). Changing the stoichiometry of **1** and [**2**]Cl from 6 : 1 to 6 : 2 and 6 : 3 also afforded the same 1 : 1 adduct as a precipitate. Similarly, the nitrate salt $[\mathbf{2}]NO_3$ in the presence of **1** also gave the corresponding 1 : 1 precipitate (Fig. S2). These results suggest that the 1 : 1 host–guest assembly possesses the lowest solubility in a local minimum state and corresponds to a metastable host–guest complex formed during the encapsulation process within the hexameric capsule. A similar 1 : 1 host–guest complex was also detected by using an elongated Ir(III) complex guest in the presence of $\mathbf{1}_6$.[12] In contrast, the PF_6 salt $[\mathbf{2}]PF_6$, which is not recognized in the cavity of **1**,[6d] gave a precipitate of pure $[\mathbf{2}]PF_6$ even in the presence of **1**, indicating that the PF_6 salt is the least soluble species in the mixture.

These results in the precipitation experiments can be reasonably explained by considering the solubilities of the molecular components. The solubili ty of the Ir(III) complex cation $[\mathbf{2}]^+$ in $CHCl_3$ is highly dependent on the counter anion. For example, the saturated $CHCl_3$ solutions of [**2**]Cl, $[\mathbf{2}]NO_3$, $[\mathbf{2}]PF_6$ reached 54, 79, and 0.43 mM, respectively (Fig. S15 and S16). This large difference is most likely due to hydrogen-bonding acceptability of the anions.[13] The ^{1}H NMR spectra of the

complex salts revealed that the Cl^- and NO_3^- ions, having a stronger hydrogen-bonding accepting ability than PF_6^-, were effectively trapped by the 3,3′-bpy moieties, leading to efficient formation of a cation–anion pair in solution (Fig. S3).[9a,14] This ion pairing effectively cancels the charge of the complex cation, thereby enhancing its solubility in apolar organic solvents such as $CHCl_3$. In a similar way, upon molecular recognition of $[\mathbf{2}]^+$ by host **1**, the counter ions were expelled from the 3,3′-bpy sites, thereby reducing the solubility of the complex cation in $CHCl_3$ and promoting precipitation of the kinetically formed 1 : 1 host–guest complex. This binding motif of the 1 : 1 host–guest structure was elucidated by ^{1}H NMR studies (Fig. S4–S7). The ^{1}H NMR spectra showed that the chemical shifts of free $[\mathbf{2}]^+$ gradually moved as the stoichiometric ratio of **1** was varied, indicating the formation of the 1 : 1 host–guest assembly prior to encapsulation. Notably, the signals of $[\mathbf{2}]^+$ showing the large shift to up-field regions corresponded to the bpy ligand. This observation can be rationalized by considering that the bpy unit is more electron-deficient than the ppy units, and is therefore recognized preferentially by the electron-rich aromatic host **1** in solution. Because the concave cavity of **1** can accommodate only one pyridine unit of the bpy ligand, the resorcin[4]arene host exhibits rapid site exchange between the two pyridine moieties of the bpy ligand in solution (Fig. S4). This binding motif of the 1 : 1 host–guest complex is consistent with the effective dissociation of the ion pair [**2**]Cl upon molecular recognition by **1**, thereby modulating the solubility of the complex cation.

Although the stoichiometry of the precipitate could be clearly determined by ^{1}H NMR analysis, the assembled structure of the precipitate remained unclear, because the powder was amorphous and featureless, as confirmed by powder X-ray diffraction analysis (Fig. S13). Therefore, we next attempted to obtain a single-crystal structure of the 1 : 1 assembly as a low-entropy, information-rich state to gain structural insight into its binding motif.[15] Although single crystals could not be obtained from a $CHCl_3$ solution, slow evaporation of a MeOH solution of $[\mathbf{2}]^+$ in the presence of **1** afforded block-shaped yellow crystals suitable for single-crystal X-ray diffraction analysis. The X-ray structure undoubtedly revealed the formation of 1 : 1 host–guest complex, in which the concave cavity of **1** bound to the bpy unit of $[\mathbf{2}]^+$ and the Cl^- ion was trapped by a hydrogen-bond (2.913(7) Å) with a hydroxy group of **1** (Fig. 3). In contrast, the X-ray structure of free [**2**]Cl visualized hydrogen bonds (3.604(9) and 3.794(9) Å) between the 3,3′-bpy moieties and the Cl^- ion (Fig. S9). These binding motifs among **1**, $[\mathbf{2}]^+$ and Cl^- are fully consistent with those proposed based on the NMR studies. Notably, in polar solvents, disassembly of $\mathbf{1}_6$ was promoted to form 1 : 1 host–guest assembly, as confirmed by NMR titration experiments in CD_3OD (Fig. S5–S7). Nevertheless, the X-ray crystallographic results clearly revealed the structural characteristics of the 1 : 1 host–guest structure, which represents the metastable structure formed in $CHCl_3$ solution.

The photophysical properties of $[\mathbf{2}]^+$ arise from mixed excited states involving triplet metal-to-ligand (^{3}MLCT) and ligand-to-ligand charge transfer (^{3}LLCT) transitions.[16] Because

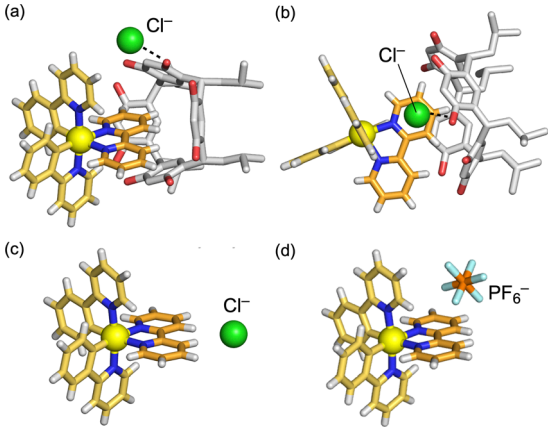

Fig. 3 Molecular structure of the complexes determined by single-crystal X-ray diffraction analysis: (a) side view and (b) view along the N–Ir–N axis of [**1**·**2**]Cl, (c) [**2**]Cl, and (d) [**2**]PF_6. [a] The bpy unit of $[\mathbf{2}]^+$ is sandwiched by the concave cavity of **1**. The chloride ion is trapped by a hydrogen bond (2.913(7) Å) with a hydroxy group of **1**. [a] ref. 17.

the charge-transfer excited states of $[\mathbf{2}]^+$ are sensitive to the surrounding environment and the lowest unoccupied molecular orbital (LUMO) of $[\mathbf{2}]^+$ is mainly localized on the bpy units, the luminescent properties of the 1 : 1 assemblies provide structural information about the local environment around $[\mathbf{2}]^+$ in the solid state (Fig. 4). The 1 : 1 assembly obtained by precipitation exhibited yellow emission (λ_{max} = 548 nm, Φ_{em} = 13%, τ_{ave} = 470 ns). In contrast, single crystals of [**1**·**2**]Cl showed a broader emission spectrum (λ_{max} = 523 nm, Φ_{em} = 35%, τ_{ave} = 500 ns). When the crystal was ground into an amorphous, featureless solid, the emission shifted to lower energy (λ_{max} = 550 nm, Φ_{em} = 13%, τ_{em} = 340 ns), displaying photophysical properties similar to those of the precipitated sample. These observations suggest that the 1 : 1 assembly obtained by precipitation adopts a molecular arrangement around $[\mathbf{2}]^+$ similar to that in the crystalline sample. Notably, the emission peaks of

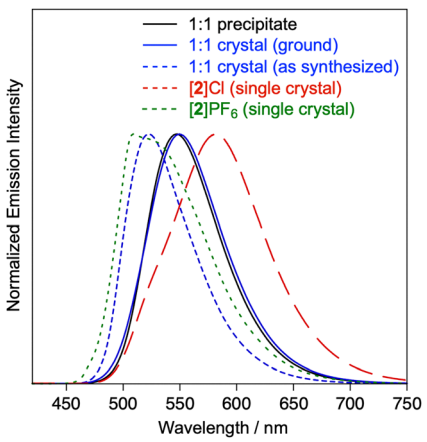

Fig. 4 Emission spectra of host–guest complexes and complex salt in the solid states (λ_{ex} = 400 nm), in which photoluminescence is derived from $[\mathbf{2}]^+$. Owing to the environment-sensitive characteristics of the excited states of $[\mathbf{2}]^+$, the emission properties of $[\mathbf{2}]^+$ gave structural information on the solid samples.

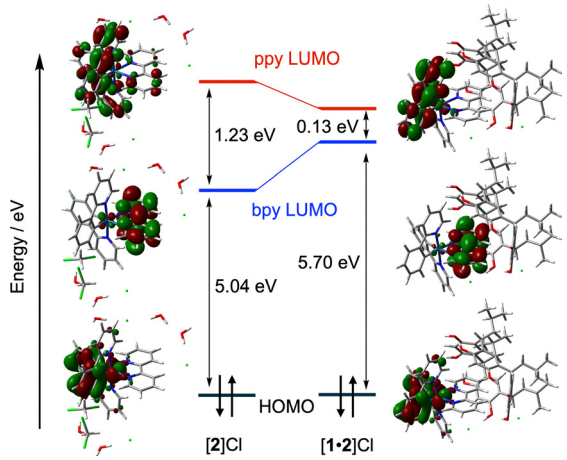

Fig. 5 Energy diagrams showing the energy levels of HOMOs and LUMOs of the ground states of $[\mathbf{2}]^+$ in the crystalline state of [**2**]Cl and [**1**·**2**]Cl.

the 1 : 1 assemblies were considerably blue-shifted compared with those of crystalline [**2**]Cl (λ_{max} = 582 nm, Φ_{em} = 7%, τ_{em} = 280 ns). In the crystal structure of [**2**]Cl, the Cl^- anion is located on the bpy plane, where it forms hydrogen bonds with the 3,3′-bpy moieties. Thus, the observed differences in emission originate from variations in the positioning of electron-rich components surrounding the bpy units of $[\mathbf{2}]^+$, which effectively modulates its LUMO level in the solid states. Indeed, the photophysical properties of crystalline $[\mathbf{2}]PF_6$ showed higher-energy emission (λ_{max} = 507 nm, Φ_{em} = 26%, τ_{em} = 520 ns) than those of the 1 : 1 assemblies, because the PF_6^- anions are positioned above the bpy ligands (Fig. 3d).[17] To further elucidate the contribution of the surrounding components to the photophysical properties of $[\mathbf{2}]^+$ in the crystalline state, quantum-mechanics/molecular-mechanics (QM/MM) calculations were examined. The calculations revealed that the LUMO levels were significantly destabilized by the presence of the electron-rich components above the bpy unit of $[\mathbf{2}]^+$ (Fig. 5). Furthermore, the unoccupied molecular orbitals of the ppy ligands contributed to the excited states of $[\mathbf{2}]^+$ in $[\mathbf{2}]PF_6$, enhancing the ligand-centered (LC) character of the excited states and vibronic structure of the emission spectrum, in good agreement with the experimental results (Fig. S20 and S22). These results clearly demonstrate that the photophysical properties of the crystalline samples reflect the structure–property relationships in these multicomponent assemblies and provide valuable structural insights into amorphous or noncrystalline solids, based on the characteristics of their crystalline forms.

In summary, we successfully isolated and characterized a metastable 1 : 1 host–guest complex composed of a concave organic host and an octahedral-shaped Ir(III) coordination complex. Crystallographic and spectroscopic analyses revealed that the bpy ligand of $[\mathbf{2}]^+$ is recognized in the concave cavity of the host, which represents a local minimum state in the encapsulation process. This study demonstrates a simple and effective protocol to capture and investigate metastable supramolecular assemblies through solubility control, providing new insights into the energy landscape of host–guest systems.

This work was financially supported by JSPS KAKENHI Grant Numbers JP23K04775, JP23H03941 (S. H.), JP20H05839 (M. H.), and by SEI group CSR Foundation. This work was supported by "Advanced Research Infrastructure for Materials and Nanotechnology in Japan (ARIM)" of the Ministry of Education, Culture, Sports, Science and Technology (MEXT), Grant Number JPMXP1223UT0168 and JPMXP1224UT0012. The computations were partly performed using the Research Center for Computational Science, Okazaki, Japan (Project: 24-IMS-C018 and 25-IMS-C019).

Conflicts of interest

There are no conflicts to declare.

Data availability

All data supporting the findings of this study are contained within the article and the accompanying supplementary information (SI). Supplementary information is available. See DOI: https://doi.org/10.1039/d5cc06960b.

CCDC 2496137 ([**1**·**2**]Cl) and 2496138 ([**2**]Cl) contain the supplementary crystallographic data for this paper.[18a,b]

References

1 J. W. Steed and J. L. Atwood, *Supramolecular Chemistry*, Wiley, 3rd edn, 2022.
2 (*a*) K. Yang, *et al.*, *Chem. Commun.*, 2018, **54**, 5911–5914; (*b*) L. Shao, *et al.*, *Angew. Chem., Int. Ed.*, 2020, **59**, 11779–11783; (*c*) X.-Y. Hu, *et al.*, *J. Controlled Release*, 2020, **324**, 124–133; (*d*) J. Li, *et al.*, *Org. Chem. Front.*, 2023, **10**, 1927–1935; (*e*) C. J. T. Cox, *et al.*, *Chem. Soc. Rev.*, 2024, **53**, 10380–10408; (*f*) S. Bhattacharyya, *et al.*, *Chem. Sci.*, 2025, **16**, 21238–21258; (*g*) J. N. Butt and L. J. C. Jeuken, *Chem. Rev.*, 2026, **126**, 1763–1791.
3 (*a*) E. Karsenti, *Nat. Rev. Mol. Cell Biol.*, 2008, **9**, 255–262; (*b*) S. O. Rizzolo, *EMBO J.*, 2014, **33**, 788–822; (*c*) H. Hess and J. L. Ross, *Chem. Soc. Rev.*, 2017, **46**, 5570–5587; (*d*) S. F. Banani and H. O. Lee, *Nat. Rev. Mol. Cell Biol.*, 2017, **18**, 285–298.
4 (*a*) S. A. P. van Rossum, *et al.*, *Chem. Soc. Rev.*, 2017, **46**, 5519–5535; (*b*) M. Weißenfels, *et al.*, *Chemistry*, 2021, **7**, 23–37; (*c*) A. Sharko, *et al.*, *Chem. Rev.*, 2022, **122**, 11759–11777; (*d*) A. Singh, *et al.*, *Nat. Rev. Chem.*, 2024, **8**, 723–740.
5 (*a*) L. R. MacGillivray and J. L. Atwood, *Nature*, 1997, **389**, 469–472; (*b*) E. S. Barrett, *et al.*, *J. Am. Chem. Soc.*, 2008, **130**, 2344–2350; (*c*) S. Fuji, *et al.*, *Langmuir*, 2020, **36**, 6222–6227; (*d*) S. Fujii, *et al.*, *J. Phys. Chem. Lett.*, 2021, **12**, 6464–6468; (*e*) I. Horin, *et al.*, *J. Phys. Chem. Lett.*, 2022, **13**, 10666–10670; (*f*) R. Capelli and G. Piccini, *J. Phys. Chem. C*, 2024, **128**, 635–641.
6 (*a*) A. Shivanyuk and J. Rebek, Jr., *Proc. Natl. Acad. Sci. U. S. A.*, 2001, **98**, 7662–7665; (*b*) M. Yamanaka, *et al.*, *J. Am. Chem. Soc.*, 2004, **126**, 2939–2943; (*c*) Q. Zhang, *et al.*, *Chem. Sci.*, 2017, **8**, 1653–1657; (*d*) S. Horiuchi, *et al.*, *Dalton Trans.*, 2023, **52**, 6604–6618.
7 (*a*) Q. Zhang, *et al.*, *Acc. Chem. Res.*, 2018, **51**, 2107–2114; (*b*) C. Gaeta, *et al.*, *Chem. – Eur. J.*, 2019, **25**, 4899–4913; (*c*) P. L. Manna, *et al.*, *Angew. Chem., Int. Ed.*, 2020, **59**, 811–818; (*d*) T.-R. Li, *et al.*, *Nat. Chem.*, 2022, **14**, 985–994; (*e*) T.-R. Li, *et al.*, *J. Am. Chem. Soc.*, 2023, **145**, 4294–4303; (*f*) G. Ferrino, *et al.*, *Chem. – Eur. J.*, 2024, **30**, e202303678.
8 H. Ichou, *et al.*, *Inorg. Chem. Front.*, 2025, **12**, 1028–1039.
9 (*a*) S. Horiuchi, *et al.*, *Dalton Trans.*, 2020, **49**, 8472–8477; (*b*) K. Uratani, *et al.*, *J. Chem. Phys.*, 2024, **161**, 201101.
10 (*a*) S. Merget, *et al.*, *J. Am. Chem. Soc.*, 2020, **142**, 4400–4410; (*b*) T. Zhang, *Chem. – Eur. J.*, 2021, **27**, 434–443; (*c*) M. Chwastek, *et al.*, *J. Am. Chem. Soc.*, 2022, **144**, 5350–5358.
11 S. Horiuchi, *et al.*, *Nat. Commun.*, 2023, **14**, 155.
12 S. Ogura, *et al.*, *ChemPhotoChem*, 2026, **10**, e202500343.

13 S. J. Pike, *et al.*, *J. Am. Chem. Soc.*, 2017, **139**, 6700–6706.
14 G. E. Schneider, *et al.*, *Dalton Trans.*, 2014, **43**, 1961–1964.
15 S. Horiuchi, *et al.*, *Nat. Commun.*, 2025, **16**, 7588.
16 (*a*) S. Ladouceur, *et al.*, *Eur. J. Inorg. Chem.*, 2013, 2985–3007; (*b*) K. P. S. Zanoni, *et al.*, *Dalton Trans.*, 2015, **44**, 14559–14573.
17 K. J. Suhr, *et al.*, *Dalton Trans.*, 2016, **45**, 17807–17823.
18 (*a*) CCDC 2496137: Experimental Crystal Structure Determination, 2026, DOI: 10.5517/ccdc.csd.cc2psfkh; (*b*) CCDC 2496138: Experimental Crystal Structure Determination, 2026, DOI: 10.5517/ccdc.csd.cc2psflj.